21st IMEKO TC4 International Symposium and
19th International Workshop on ADC Modelling and Testing
Understanding the World through Electrical and Electronic Measurement
Budapest, Hungary, September 7-9, 2016

CT based analysis of reworked BGA devices

I. Fekete[1,a], I. Kozma[1,b], R. Csontos[2,c]

[1]Széchenyi István University, Audi Hungaria Faculty of Automotive Engineering, Department of Material Sciences and Technology, H-9026 Hungary, Győr, Egyetem tér 1.
[2]iQor Global Services Hungary Kft, H-9700 Hungary, Szombathely, Vásártér u. 1
[a]fekeim@sze.hu, [b]kozma@sze.hu,[c]robert.csontos@iqor.com

***Abstract* – The widespread use of computed tomography in the electronic field allows for an extended range of measurements to be carried out. High integration devices can be tested easily with µCT, and provide large amount of data to characterize the technology parameters. This paper focuses on the inspection of BGA solder ball geometry and quantification of different properties of the solder arrays.**

***Keywords* – BGA soldering, µCT**

I. INTRODUCTION

CT-based reconstruction methods are used successfully in many different materials research fields such as the research of porous polymeric materials (foams) [1], open celled and closed-cell metallic foams [2-3]. Recently X-ray computed micro tomography has been applied on porous fuel cell materials [4] and soil samples [5]. The history, the production, the geometrical, mechanical, thermal properties, the dynamical behaviour and the fatigue processes of hollow spheres were studied in details [6]. Structural characterisation and morphology of metal foams were studied with models reconstructed from CT images [7]. CT and MRI reconstruction methods were developed in the case of liquid foams [8-9], as well.

With the increasing demand for smart phones and tablet computers the electronic parts making up these devices must be of best quality. Large scale integration with Ball Grid Array (BGA) devices is common in this segment. Repair of these devices often requires the rework of the BGA components.

BGA devices are surface mount integrated circuit packages designed to have large connection density, up to many hundreds of pins Fig. 1. The connections are usually of a ball shape solder joints that provide good high speed electrical properties.

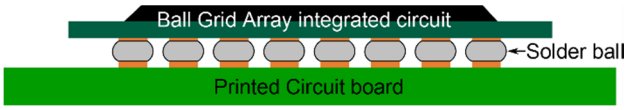

Fig. 1.: Schematic cross section of a BGA device soldered on to a printed circuit board.

Reworking is a process of desoldering the Integrated Circuit (IC) and soldering a new or previously desoldered IC on the Printed Circuit Board (PCB). Re-soldering involves the heating of the PCB to the melting point of the solder, following a thermal profile to achieve a good solder joint.

Because of the nature of the rework process, it cannot be fully automated, and must be carried out by skilled operators. Rework parameters must be followed strictly in order to produce the same quality soldering on every device.

The metallurgical processes [10], the materials [11] and the testing methods [12] of the BGA soldering were studied earlier.

In this paper smart phone PCBs were reworked and were scanned using an industrial Micro Computed Tomography (µCT), then the reconstruction data was used to extract the geometry of the solder balls. A software developed in this work was used to analyse the extracted geometry to provide useful information on the quality of the solder balls.

II. ANALYSIS METHOD

Rework parameters for the sample smartphone PCBs were the following: reflow peak temperature was increased by 30°C above the optimal, reflow peak temperature was decreased by 10°C below the optimal, soldering was done without using flux, rework was done two times on the device.

Scans were carried out with an YXLON Modular CT system equipped with a 225kV micro focus X-ray tube and an Y.XRD1620 detector. The tube was operating at 200kV tube voltage and 0.12mA tube current, no filters were used. The detector was set to a 2x2 binning mode

resulting in a 1024x1024 pixel resolution, the integration time was set to 1000ms, 1440 projections were taken.

The narrow geometry of the sample PCBs allowed for a good magnification of the BGA devices, reaching a voxel resolution of 28.4 µm.

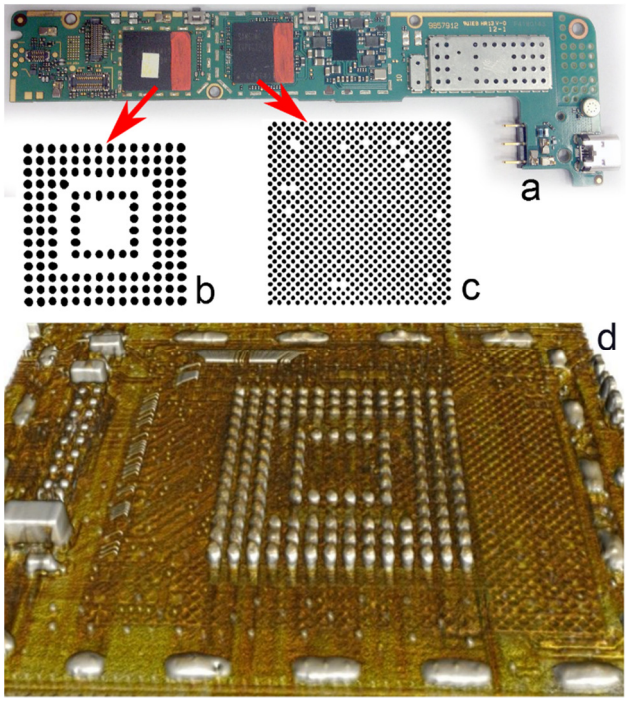

Fig. 2.: The inspected PCB (a) with the 2 reworked BGA devices: one with a low pin-count footprint (b) and one with a high pin-count footprint (c). µCT based 3D reconstruction of one of the BGA package (d)

The scan slices were loaded into VGStudio MAX for surface extraction, no filter was applied to the data. Automatic surface determination was executed on the volume. This process sets an iso-value that is used to distinguish between material and air in the volume. The automatic surface determination finds the peak of the material and air components in the histogram, and sets the iso-value to the mean of these two peaks [13].

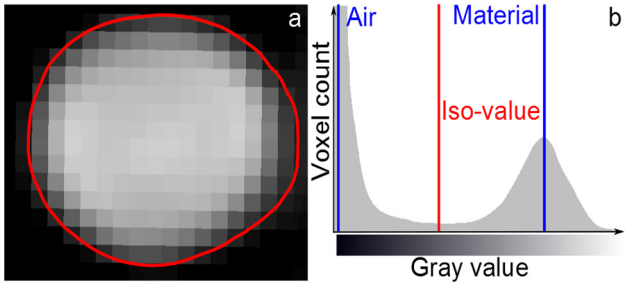

Fig. 3.: Determined surface on a volume slice (a) and the histogram (b) that shows the air and material components with the determined iso-value.

The iso-value is used to determine the iso-surface of the material, which is a continuous surface that embodies the material in the volume.

Triangle mesh was extracted from the solder balls iso-surface. The mesh quality in the software was set to a predefined setting called "precise", which sets the point resampling distance to 0.14 mm and the point reduction tolerance to 0.07 mm. The point resampling means that the software samples the iso-surface at the given distances. Point reduction removes the sampled points if they are within a given tolerance in order to reduce the size of the mesh.

The extracted mesh is used by the software we developed to produce the analysis of the data. The following properties are calculated for the solder balls: volume, diameter, sphericity, smallest distance between the neighbouring balls, projected area.

III. ANALYSIS RESULTS

Volume calculation of the solder balls were done according to [14]. For each triangle in the mesh we connect the triangle vertices to a point, thus creating a tetrahedron. The point we connect the vertices to is the center mass of the solder ball, so the aspect-ratio of the tetrahedron is optimal. This center mass is the origin for the calculation of the volume. The volume of the mesh can be calculated from an equation (1).

$$V = \sum_i \frac{1}{6}(-x_{i3}y_{i2}z_{i1} + x_{i2}y_{i3}z_{i1} + x_{i3}y_{i1}z_{i2} - x_{i1}y_{i3}z_{i2} - x_{i2}y_{i1}z_{i3} + x_{i1}y_{i2}z_i) \quad (1)$$

Where V is the volume of the triangle mesh, i is the index of the triangles, x, y and z are the coordinates of the triangle vertices. The second subscript indicates the vector of the triangle.

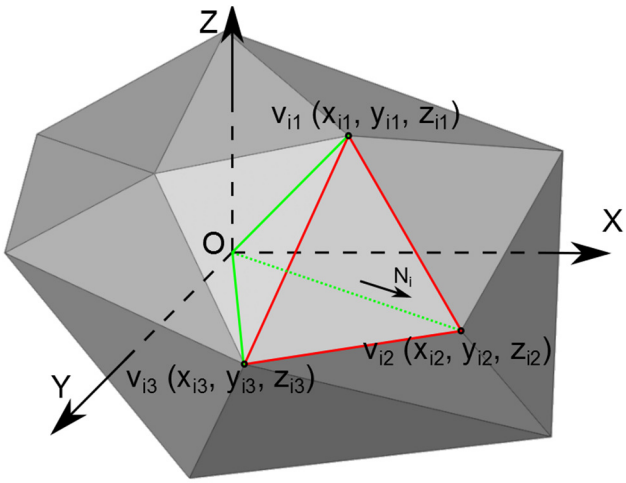

Fig 4.: Calculation of tetrahedron volume form the triangle mesh. Red lines show the triangle outline, green lines show the triangle vertices connected to the origin.

The surface calculation of the mesh was done by calculating the cross product of two vectors of the triangles. The length of a cross product is the area of the triangle. The following images show the top view of the triangle meshes of the solder balls colormapped according to various properties. The colorbars range from the lowest to the highest value of the property. The distributions of the properties are displayed on the colorbar, mean values are also indicated on the histogram.

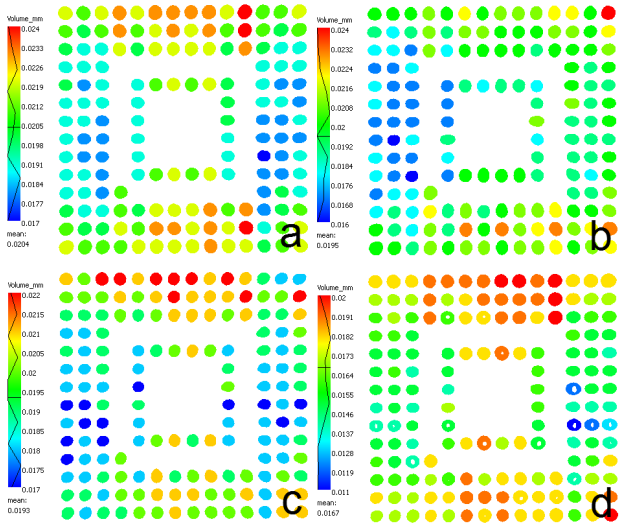

Fig. 5. Analysis result of the solder balls, the coloring of the footprint shows the calculated volume of the solder balls. Reference device (a), device with reflow temperature +30°C (b), device reflow without flux (c), device replaced two times (d).

According to our calculations the values of the ball volumes range from 0.17mm^3 to 0.024mm^3, Fig. 5. The reference device has larger mean solder ball volume than the reworked devices. In Fig.5.d. solder balls having holes in their centers can be observed. These holes are so large voids that they are penetrating the top and bottom of the solder balls.

Sphericity of the solder balls was calculated with the following equation:

$$S = \frac{\pi^{\frac{1}{3}}(6V)^{\frac{2}{3}}}{A}, \qquad (2)$$

Where S is the sphericity, V is the volume and A is the surface of the triangle mesh.

The shapes of the solder balls are not perfect spheres, the measured sphericity never reaches 1, as can be seen on the colorbars. However this property can be used to comparatively quantify the shapes of the solder balls within a group of set technological parameters.

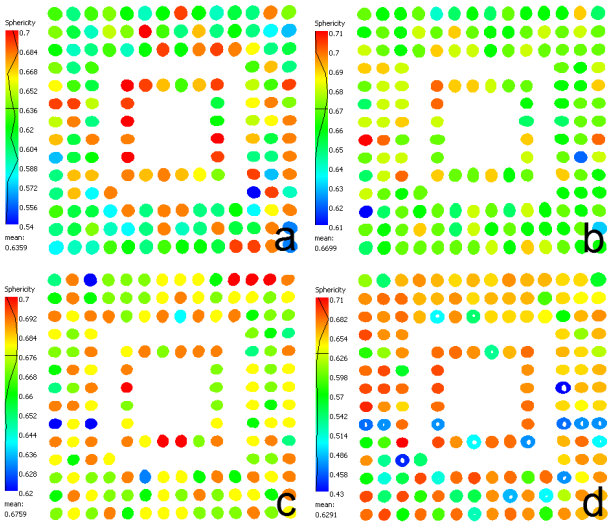

Fig. 6. Analysis result of the solder balls, the coloring of the footprint shows the calculated sphericity of the solder balls. Reference device (a), device with reflow temperature +30°C (b), device reflow without flux (c), device replaced two times (d).

Fig. 6. shows the sphericity of the solder balls. One can observe the distributions on the colorbar and see that the reference device has larger deviations in sphericity than the reworked devices. In Fig. 6.d. the hollow solder pads show the worst sphericity.

Solder ball diameters were calculated which can be seen in Fig. 7. The device reflowed at a higher +30°C temperature shows smaller diameter distribution than the other devices.

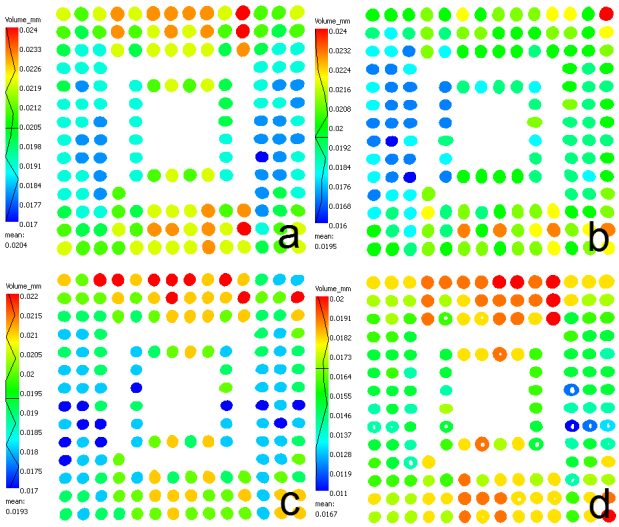

Fig. 7. Analysis result of the solder balls, the coloring of the footprint shows the diameter of the solder balls. Reference device (a), device with reflow temperature +30°C (b), device reflow without flux (c), device replaced two times (d).

Distances between the neighbouring solder balls were also calculated, the smallest distances are shown in Fig. 8. The device replaced two times shows signs of greater neighbouring distance compared to the other devices. The distribution of the distances shown on the colorbar proves that the device replaced two times has the smallest standard deviation, so the patterning of the solder balls is the most even here.

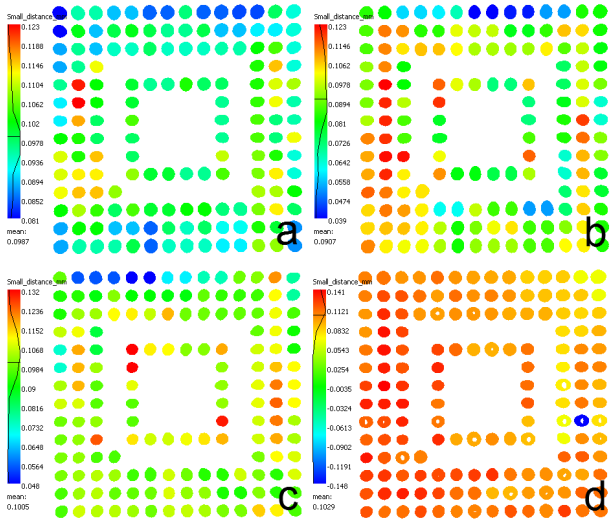

Fig. 8. Analysis result of the solder balls, the coloring of the footprint shows the smalles distance to the neighbouring solder ball. Reference device (a), device with reflow temperature +30°C (b), device reflow without flux (c), device replaced two times (d).

Projected areas were calculated in the X, Y and Z directions. Fig. 9. shows the projected areas of the solder balls in the X direction. The reference device shows that the solder balls in the middle have smaller area than the ones on the perimeter. This is caused by the bending of the device during cooling. The cold soldered device has multiple coalesced solder balls in groups of 2 and 3, Fig. 9.b. This results in an increased projected area so the range of the colorbar is expanded more than in the case of the reference device.

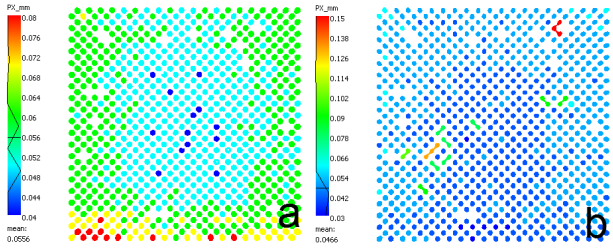

Fig. 9. Analysis result of the solder balls, the coloring of the footprint shows the projected area of the solder balls. Reference device (a), cold soldered device -10°C (b).

Principal Component Analysis (PCA) [15] was applied to the solder ball mesh data to calculate the length of the principal component axes, shown in Fig. 7. The coalesced solder balls of the cold soldered device have the greatest principal axis lengths.

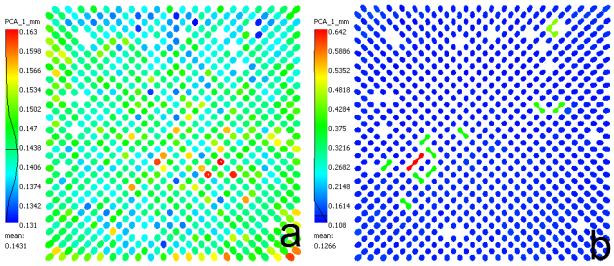

Fig. 10. Analysis result of the solder balls, the coloring of the footprint show the first principal axis length of the solder balls.. Reference device (a), cold soldered device -10°C (b).

IV. CONCLUSION

In this case study we showed that the computed tomography reconstruction can provide large amount of information about the BGA solder properties, even more information than the conventional X-ray radiography methods.

Both the quantitative geometric properties (e.g. volume, diameter, smallest distance) and the shape properties (e.g. sphericity, projected area, PCA axis length) allow for a detailed analysis of the solder balls. These useful information can provide a good analysis of the rework technology parameters.

V. ACKNOWLEDGEMENT

This research has been supported by the „Highly industrialized region on the west part of Hungary with limited R&D capacity: Research and development programs related to strengthening the strategic future oriented industries manufacturing technologies and products of regional competences carried out in comprehensive collaboration" program of the National Research, Development and Innovation Fund (NKFI), Hungary, Grant. No. VKSZ_12-1-2013-0038.

REFERENCES

[1] Léonard A., Calberg C., Kerckhofs G., Wevers M., Jérome R., Pirard J.P., Germain A., Blacher S.J., Porous Mater. 2008;15:397-403.

[2] Vicente J., Topin F., Daurelle J.V., Materials Transactions 2006;47:2195-2202.

[3] Jeon I., Katou K., Sonoda T., Asahina T., Kang K.J., Mechanics of Materials 2009;41:60-73.

[4] Wargo E.A., Kotaka T, Tabuchi Y, Kumbur EC, J. of Power Sources 2013;241:608-618.

[5] Houston A.N., Schmidt S., Tarquis A.M., Otten W., Baveye P.C., Hapca S.M., Geoderma 2013;207-208:154-165.

[6] Oechsner A., Augustin C., Multifunctional Metallic Hollow Sphere Structures, Springer, 2009

[7] Vesenjak M., Borovinsek M., Fiedler T.: Structural characterisatition of advanced pore morphology (APM) foam elements, Materials Letters, 2013;110: 201-203

[8] Vasconcelos I.F., Cantat I., Glazier J.A.: Dynamics and topological aspects of a reconstructed two-dimensional foam time series using Potts Model on a pinned lattice, Journal of Computational Physics 192, 2003, pp. 1-20.

[9] Zsoldos I.: Reconstruction method of foam structures from MRI imaging, In: Misra SC.: Recent Advances in System Science and Simulation in Engineering: 435 p., WSEAS Press, 2008. pp. 168-172. ISSN: 1790-2769.

[10] Jeong-Won Yoon, Sang-Won Kim, Seung-Boo Jun: Effect of reflow time on interfacial reaction and shear strength of Sn–0.7Cu solder/Cu and electroless Ni–P BGA joints. Journal of Alloys and Compounds 385 (2004) 192–198

[11] W.H. Zhong, Y.C. Chan, M.O. Alam, B.Y. Wu, J.F. Guan: Effect of multiple reflow processes on the reliability of ball grid array (BGA) solder joints. Journal of Alloys and Compounds 414 (2006) 123–130

[12] Mohammad S. Laghari, and Qurban A. Memon: Identification of Faulty BGA Solder Joints in X-Ray Images. International Journal of Future Computer and Communication, Vol. 4, No. 2, April 2015

[13] Cha Zhang and Tsuhan Chen: Efficient feature extraction for 2D/3D objects in mesh representation

[14] Volume Graphics GmbH: VGStudio MAX Reference Manual, 2012

[15] Steven M. Holland: Principal components analysis (PCA)